Mitochondrial effects on fertility and longevity in *Tigriopus californicus* contradict predictions of the mother's curse hypothesis

SUMMARY

Strict maternal inheritance of mitochondria favors the evolutionary accumulation of sex-biased fitness effects, as mitochondrial evolution occurs exclusively in female lineages. The "mother's curse" hypothesis proposes that male-harming mutations should accumulate in mitochondrial genomes when they have neutral or beneficial effects on female fitness. Rigorous empirical tests have largely focused on *Drosophila*, where support for the predictions of mother's curse has been mixed. We investigated the impact of mother's curse mutations in *Tigriopus californicus,* a minute crustacean. Using nonrecombinant backcrosses, we introgressed four divergent mitochondrial haplotypes into two nuclear backgrounds and recorded measures of fertility and longevity. We found that the phenotypic effects of mitochondrial mutations were context-dependent, being influenced by the nuclear-background in which they were expressed, as well as the sex of the individual and rearing temperature. Mitochondrial haplotype effects were greater for fertility than longevity, and temperature effects were greater for longevity. However, in opposition to mother's curse expectations, females had a higher level of mitochondrial genetic variance than males for both fertility and longevity, and there was no evidence for mitochondrial mutations favoring female performance at the cost of male performance. These results indicate that selection has not resulted in the accumulation of male mutation load in *Tigriopus californicus*.

22

23 # Introduction

24 In eukaryotes, life is powered by mitochondria - cytoplasmic organelles capable of producing
25 energy in the form of ATP. Originating from an ancient symbiosis over 2 billion years ago,
26 mitochondria provided the energy required for the evolution and diversification of multicellular
27 organisms[1–3]. Over evolutionary history, mitochondrial genomes have retained their ancestral
28 genetic codes and a few dozen genes while dramatically reducing their genome size through
29 deletion and gene transfer to the nucleus. Beyond the generation of ATP by oxidative
30 phosphorylation (OXPHOS), mitochondria perform additional cellular functions, including
31 initiation of apoptosis, amino acid and steroid biosynthesis, β-oxidation of fatty acids, cellular
32 signaling, and nuclear epigenetic regulation [4–8]. Nevertheless, out of 1,500 or more proteins
33 found in the mitochondrion, only the 13 membrane-bound ETC complexes are encoded by the
34 mitochondrial genome, with the rest being encoded by nuclear DNA[9,10]. The coevolution of
35 mitochondrial and nuclear genomes is thus an ancient yet ongoing process, involving the
36 evolutionary fine-tuning of various molecular interactions (i.e. protein-protein, protein-DNA,
37 and protein-RNA) required for the accurate replication and transcription of mtDNA, translation
38 of mtDNA-encoded proteins, and efficient cellular respiration. Mutation rates are generally
39 higher in mtDNA than in nDNA[11,12] leading to a continuous introduction of new mitochondrial
40 alleles. With asexual transmission and lack of recombination in mitochondria, novel alleles are
41 likely to persist, even when slightly deleterious, due to the potential masking effect of linkage
42 disequilibrium on mitochondrial genetic variation and reduced efficacy of natural selection[13].
43 Nevertheless, mtDNA likely experiences recurrent adaptive evolution via selective sweeps acting
44 on traits such as respiratory efficiency and mitonuclear coadaptation[14–18]. In natural populations,

45 mitochondrial fitness variation is likely to be present at substantial levels and may make a
46 meaningful contribution to adaptation and diversification[19]. The distribution of fitness effects
47 among mtDNA mutations is also likely to differ between the sexes, owing to the maternal
48 inheritance of mitochondria[20–22]. Strict maternal inheritance favors the evolutionary
49 accumulation of sex-biased fitness effects, as it is expected to preclude any opportunity for
50 evolution in males, forming a sex-specific selective sieve.

51 Under maternal inheritance, mitochondrial evolution is thought to be restricted to female
52 lineages, leading to the accumulation of male-harming mutations when they have neutral or
53 beneficial effects on female fitness (i.e. "mother's curse"[21,23]). Initial evidence for the mother's
54 curse hypothesis (MCH) centered on evidence that sperm motility in humans and other taxa was
55 linked to mitochondrial function[24,25,23] therefore sperm are more exposed to deleterious effects
56 of mtDNA mutations than ova. The MCH has also been proposed to impact viability, and even to
57 contribute to the taxonomically widespread pattern of shorter male lifespans[26]. Theoretical work,
58 however, shows that conditions favoring the spread of mother's curse mutations can be limited
59 by even modest levels of inbreeding and kin selection, allowing for an adaptive response to
60 mtDNA alleles impacting male viability and fertility[27–29]. Nevertheless, interest in MCH has
61 increased steadily in recent years leading to formal tests of the hypothesis, mostly in *Drosophila*,
62 utilizing carefully constructed mitochondrial-nuclear (mitonuclear) hybrids with divergent
63 mtDNA haplotypes backcrossed into an isogenic nuclear background. The most direct test of
64 MCH focuses on the effects of mutational variation in mtDNA, which are predicted to confer
65 larger trait variance in males. A second major prediction focuses on the subset of alleles that are
66 directly sexually antagonistic, which could lead to a negative intersexual genetic correlation
67 across haplotypes. A third prediction is that experimental disruption of mitonuclear coadaptation

68 will be more detrimental to males than females. Studies using the mitonuclear hybrid approach
69 have shown both support[26,30–34], and rejection[35–38] of the mother's curse hypothesis.
70 Understanding the pervasiveness of mother's curse is crucial given its fundamental
71 implications for the evolution of sexual dimorphism, as well as very practical consequences for
72 conservation breeding programs and medicine (particularly mitochondrial replacement theory
73 and male-biased mitochondrial disease). While past work has focused on *Drosophila*, the
74 predominance of maternal inheritance of mitochondria in eukaryotes allows for a taxonomically
75 diverse investigation of the generality of mother's curse. Here we test predictions of the MCH
76 using the splash-pool copepod *Tigriopus californicus*, an arthropod that shares a common
77 ancestor with *Drosophila* at least 450 million years ago. We used a genetic panel of mitonuclear
78 hybrids to assay both fertility and longevity. As fertility genes are likely sex-specific and
79 viability genes are likely shared between the sexes (see review[39]), we predict that mitonuclear
80 mismatch will lead to stronger sex bias for fertility than longevity. Additionally, we measured
81 the impact of high environmental temperature on these traits, as mild mitonuclear mismatch can
82 be expected to be unmasked under higher metabolic demand[40]. Populations of *T. californicus*
83 show extreme genetic divergence over short geographical distances[41–43] while remaining
84 somewhat tolerant of hybridization, producing viable and fertile offspring[44,45]. Nucleotide
85 divergence in *T. californicus* extends across the mtDNA genome, involving coding and
86 noncoding genes, and can exceed 20% between distant populations. *T. californicus* also differ
87 from most model organisms in that they lack heteromorphic chromosomes - sex is determined by
88 the inheritance of multiple, unlinked genes in combination with environmental effects (polygenic
89 sex determination)[46–48]. While rarely utilized in evolutionary biology, polygenic sex
90 determination provides an advantage for testing sex-specific mitochondrial effects as sex

differences cannot be attributed to the effects of sex chromosomes. Importantly, despite the lack of heteromorphic sex chromosomes, there is marked sexual dimorphism in *T. californicus* and considerable evidence for sex-specific effects in multiple traits (thermal tolerance[49,50]; salinity tolerance[51,52]; resistance to toxins[52]; intrinsic hybridization stress[47]) in which males are generally the weaker sex.

Methods

Population sampling

Populations of *T. californicus* are distributed in supralittoral "splash pools" along the Pacific coast of North America. Copepods were originally collected from supralittoral pools at four locations (Figure 1A): Friday Harbor, WA (FHL: 48.55 N,123.01 W), La Jolla, CA (LJ: 32.83 N,117.27 W), Bird Rock, CA (BR: 32.82 N,117.27 W), and San Diego, CA (SD: 32.7460 N,117.2551 W). Isofemale lines were initiated from a single female fertilized by a single male, and maintained at 20°C on a 12h:12h light:dark cycle in standard culture media (three times filtered seawater from Wrigley Marine Science Center, Santa Catalina Island, CA; 0.1g/l of Spirulina (BRAND) and 0.1g/l ground Tetramin (Tetra®) Tropical fish food flakes). All lines were maintained in petri dishes for ≥ 5 years under these conditions and periodically fed additional Spirulina and ground Tetramin® tropical fish food and rehydrated with DI water whenever necessary to maintain approximately 35 ppt salinity. Prior to experimentation, we sequenced samples from each isofemale line at the 12S ribosomal RNA locus (Forward primer: CCAAGATACTTTAGGGATAACAGC; Reverse primer: CTGTTCTATCAAAACAGCCCT; fragment size: 687 base pairs) to rule out cross-contamination.

114 **Mitonuclear hybrid panel**

115 In *Tigriopus*, meiosis is chiasmatic in males but achiasmatic in females, yielding recombinant
116 sperm and non-recombinant ova. This allows us to backcross mitochondria from the population
117 of the dam into that of the sire while preventing nuclear recombination between populations.
118 Because sexes in *T. californicus* are not easily distinguished before maturity, we allowed males
119 to clasp female siblings with their geniculate first antennae in order to ensure the sex of females.
120 We moved clasped pairs onto filter paper and quickly separated them using entomological pins
121 under a microscope. We backcrossed FHL, BR, LJ, and SD dams to SD and BR sires for 10
122 generations (Figure 1B), resulting in an average proportion of $1 - \frac{1}{2}^{(b+1)}$ (where b is equal to the
123 number of backcross generations) or 99.95% of the sire's nuclear genome, assuming no
124 selection. For each cross, we established 4 replicates, each maintained in 12-well plates
125 containing standard culture media. All crosses were fed weekly with additional Spirulina and
126 ground Tetramin® fish food and rehydrated with DI water whenever necessary to maintain
127 approximately 35 ppt salinity.

128

129 **Trait measurement and modeling**

130 For each of our mitonuclear hybrid lines, we measured three fitness components (fertility,
131 lifespan, and age-specific rate of survival) for males and females reared at two contrasting
132 temperature regimes (15ºC and 25ºC). In order to achieve an adequate sample size for each
133 mtDNA haplotype and sex, it was necessary to set up multiple families from each mitonuclear
134 hybrid line. Each family was composed of up to four clutches of fertilized eggs derived from a
135 single mitonuclear hybrid or control female (dam). Dams were maintained at standard conditions
136 and checked daily for the presence of hatched eggsacs. For each dam, we alternated moving up

137 to four hatched eggsacs to 15ºC and 25ºC (Figure 1B) so that clutch order was orthogonal to
138 temperature in both fertility and longevity experiments. Individuals were maintained at the same
139 temperature for the duration of the fertility or longevity experiment.
140
141 **Longevity**
142 Individual animals were separated into wells in a 24-well plate once they developed to the
143 juvenile copepodid stage and were checked three times a week. The first measurement we
144 recorded was the sex-specific age of reproductive maturity. For males, this occurred with the
145 development of geniculate first antennae (claspers) and for females with the development of
146 eggs, which can be seen through the translucent body. We continued monitoring longevity
147 experiments three times a week, recording the age of death of individuals until all had expired.
148
149 We performed linear mixed-effects modeling on family sex ratio using sex information
150 from our longevity experiment, comparing mtDNA x nDNA interactions with the impact of
151 mitonuclear status on family sex ratio. We also conducted a separate experiment, using different
152 families, measuring mortality occurring before sexual maturity (Document S1, Figure S1). We
153 were able to measure the age at the naupliar-copepodid transition, duration of the copepodid
154 stage, and the sex-specific age of reproductive maturity, and perform linear mixed-effects
155 modeling investigating the influence of genetic (mtDNA, nDNA) and environmental
156 (temperature) influence on these larval life-history parameters.
157

158 **Sex-specific fertility**

159 For female fertility experiments, all individuals from hatched eggsacs were separated into
160 individual wells in a 24-well plate once they developed to the juvenile copepodid stage. To each
161 well, we added a single wild-caught adult male from the appropriate locality (SD or BR),
162 matching the paternal line of the individual. Males were added to every well because sexes are
163 difficult to distinguish morphologically in immature *T. californicus* and we wanted to ensure that
164 each female was paired with an adult male before sexual maturity. Mate clasping typically occurs
165 between adult males and juvenile females, and rarely occurs with mature females once they
166 begin extruding non-fertilized eggsacs. We also ran experiments utilizing sib-pairs in parallel to
167 compare the impact of mating with mitonuclear hybrid males versus wild-type males on female
168 fertility (Document S1). Plates were maintained at the appropriate temperature (15ºC or 25ºC)
169 and checked three times a week until females produced an eggsac. As we utilized several
170 hundred plates in our experiment, it became necessary to maximize incubator space. Therefore,
171 we placed gravid females from the same family and clutch together in petri dishes until they
172 reached experimental age. Because individuals develop twice as fast at 25ºC as at 15ºC, we used
173 temperature-specific ages for our experiment in order to minimize age-related variation. Once
174 individuals reared at 25°C reached 35 days of age, and individuals reared at 15°C reached 70
175 days of age, we moved them into separate dishes and maintained them at the correct temperature,
176 checking them three times a week until eggsacs hatched. Upon hatching, each individual larval
177 nauplius was counted under a dissecting microscope to measure female hatching number.

178 For male fertility experiments, we removed males from each of the four clutches in a
179 family and allowed them to age for the appropriate temperature (35 days old for 25ºC and 70
180 days old for 15ºC). Once at the appropriate age, each male was pipetted into a petri dish with six

181 wild-caught juvenile females from the appropriate locality (BR or SD) to match the paternal
182 nuclear line. To ensure that wild-caught juveniles were female, we selected clasped pairs from
183 culture within 0-2 weeks of collection and separated pairs under a dissecting microscope. Care
184 was taken to provide males with females of consistent and reasonably large size, to reduce
185 variation across experiments. Each experimental male and six wild-caught females were allowed
186 14 days to mate in a petri dish at the appropriate temperature. After 14 days, females were
187 isolated into a 6-well plate and scored for the presence or absence of any offspring indicating a
188 successful mating. We recorded male remating success as the ratio of successful matings to the
189 number of surviving females.
190

191 **Parametric and nonparametric trait modeling**

192 For our trait modeling, we performed three types of linear models: sex-effect modeling,
193 coevolutionary status modeling, and best-fit models. Sex-effect models measure sex effects
194 impacted by mtDNA and nDNA variation and their interactions. If mother's curse mutations are
195 present, they may exist in additive (Sex x mtDNA) or epistatic (Sex x mtDNA x nDNA) form.
196 Sex differences may also be encoded by nuclear genes, described by the (Sex x nDNA) term. In
197 order to compare fertility experiments across the two sexes, individual measurements of fertility
198 were normalized to the mean of the appropriate matched control line reared at the same
199 temperature: (x_i/m_x). We performed model testing on the four sex-effect models using the
200 *model.sel* function in the MuMIn[53] R package, which ranks models based on their AIC_C values.
201 Model contrasts for sex differences were performed using the *pairs* function from the emmeans[54]
202 R package . Coevolutionary status models measure the impact of disrupting coevolved
203 mitonuclear combinations on sex-specific data grouped by temperature and nDNA. These

204 models included coevolutionary status as a fixed-effect term. Modeling for best-fit utilized an
205 "all-subset" approach, where all possible combinations of predictors were compared using the
206 *MuMIn* functions *dredge* and *model.avg*. Models with the highest weight and lowest AIC_C were
207 designated as best-fit. Longevity best-fit models included temperature, sex, nDNA, mtDNA and
208 all possible interactions as fixed-effects terms in initial models, while fertility model selection
209 was performed on sex-specific models without the sex term. All linear mixed-effects modeling
210 was performed using the *lmer* function from the lme4[55] R package and included clutch nested
211 within family as a random-effect term. We used type III ANOVA to estimate significance for
212 model main effects and interaction terms using the *Anova* function from the car[56] R package.
213 We performed parametric regression of survivorship for each nuclear, temperature, and
214 sex combination against the Gompertz distribution [57], estimating the shape (α) and rate (β)
215 parameters using the R package flexsurv[58]. Parameters were estimated by maximum likelihood,
216 with those defined to be positive estimated on a log scale. Confidence intervals were estimated
217 from the Hessian at maximum, and then transformed back to the original scale (days). The shape
218 of the resulting distributions, ln(α), describe the initial mortality rate or frailty of the samples,
219 while the rate (β) parameter describes the age-independent rate of mortality acceleration or rate
220 of senescence. We employed Kruskal-Wallis one-way analysis of variance to estimate the
221 significance of parameter estimates produced by parametric survival models using the
222 *kruskal.test* function from the stats[59] R package.
223

224 **Mitochondrial coefficient of variation**

225 One prediction of the mother's curse hypothesis is that the accumulation of male-affecting
226 variation should lead to a higher mitochondrial coefficient of variation (CV_{mt}) in males than in

227 females. Using the *boot*[60,61] package in R, bootstrapped CV_{mt} was computed by resampling raw
228 trait means for each mitochondrial line using 1000 replicates with replacement and calculating
229 the coefficient of variation among mitochondrial lines ($CV = \sigma/\mu$) for each nuclear, sex, and
230 temperature combination. Hypothesis testing was performed to compare male and female CV_{mt}
231 using a sign test as implemented in the *SIGN.test* function in the BSDA[62] R package.

232

233 **Genetic correlation among haplotypes**

234 Mother's curse mutations are likely to reach fixation fastest when they confer a fitness advantage
235 to females, resulting in sexual conflict when they simultaneously result in low fitness in males.
236 When enough mtDNA variation is involved in sexual conflict, a negative intersexual correlation
237 may be observed across haplotypes for a given trait. We measured the correlation between
238 haplotype means for fertility and median longevity, comparing traits within sexes (intrasexual
239 correlation) and also comparing the sexes for a given trait (intersexual correlation). We used
240 bootstrapped estimates of Pearson's coefficient using the boot R package along with the *cor*
241 function from the stats R package, recording 1000 samples for each comparison. Equi-tailed,
242 two-sided nonparametric confidence intervals were generated from the first order normal
243 approximation with a confidence level of 0.95 using the *boot.ci* function from the boot package
244 in R.

245

246 **Whole genome sequencing**

247 For each isofemale and mitonuclear hybrid line, we extracted DNA from 10 males and 10
248 females using Zymo quick-DNA preps and quantified DNA yields using Qubit HS dsDNA

249 quantification kits. Because female *T. californicus* yield approximately 2.12x more DNA than
250 males, we pooled 2 ng of DNA from each of the 20 individuals per line for library preparation.
251 DNA pools were sheared using a Covaris S2 sonicator with microTUBE-50 AFA tubes, and
252 sequencing libraries were prepared using Qiagen QIAseq Ultralow Input kits following
253 instructions. Mitonuclear hybrid libraries were pooled together in equimolar amounts and
254 sequenced together on a single lane of Illumina HiSeq4000 (PE-150), and the parental isofemale
255 libraries were pooled and sequenced on a separate lane. Sequence reads were quality trimmed
256 using trimmomatic[63] v0.36, and paired reads were filtered for mitochondrial reads using the
257 filter_reads.pl perl script included with the NOVOPlasty[64] software. We assembled consensus
258 mtDNA genomes from each sequenced isofemale line, by utilizing the appropriate mtDNA
259 reference from a previous publication which included the SD, BR, and FHL populations[18]. A
260 reference mtDNA genome did not exist for the LJ population, so those reads were mapped to the
261 BR mtDNA reference. We annotated our *de novo* assembled genomes using the Mitos[65] 2.0
262 software, each containing all 13 protein coding genes, and the majority of non-coding RNAs.
263 Following this, we mapped all trimmed and paired reads to the *T. californicus* reference genome
264 assembly (NCBI accession: GCA_007210705.1) along with the appropriate mitochondrial
265 genome using stampy[66] v1.0.32 (substitutionrate=0.05). Following the removal of PCR and
266 optical duplicates using picard[67] MarkDuplicates, we called variants for each sequenced pool
267 using samtools[68] mpileup.

268 We estimated pairwise nuclear divergence for isofemale lines in a sliding window
269 approach. For each comparison, we calculated F_{ST} using a sliding window of 10,000 bp,
270 requiring a depth of 40x coverage, and minimum PHRED base quality score of 30 using the fst-
271 sliding.pl perl script included with popoolation v1.2.2. For parental mitochondrial divergence,

272 we aligned whole mtDNA genomes using progressiveMauve[69] along with mtDNA genome
273 sequences from an outgroup population from San Roque, Baja California Sur, Mexico to produce
274 rooted trees, and measured divergence (d_{XY}) using the calculate-dxy.pl perl script included with
275 popoolation v1.2.2. We also measured divergence at synonymous and nonsynonymous sites by
276 aligning protein-coding sequences with MACSE [70] v2, constructing neighbor joining trees with
277 ClustalW [71] and analyzing these data with codeml from the PAML suite [72] using the null model
278 (M0), assuming a uniform selective pressure among sites.
279

280 **Confirming mitonuclear genetic status of hybrids**

281 To test for potential selection or accidental introgression, we measured allele frequencies at a set
282 of divergent sites for each paternal line's nuclear genome. A Fisher's exact test for significant
283 allele frequency differences for nDNA from the maternal and paternal lines was conducted using
284 popoolation[73] v1.201, requiring a minimum depth of 20x coverage. In mitonuclear hybrids, sites
285 with no significant differences (alpha > 0.05) to the paternal line were considered "paternally
286 concordant" and significantly different sites (alpha <= 0.05) were considered "paternally
287 discordant". Because significance may be determined by variations in the same alleles between
288 lines, we recorded paternally discordant sites with alleles matching maternal lines as "maternally
289 concordant" when they were absent in the paternal nDNA. Paternal concordance rates were
290 recorded by measuring the proportion of sites that were not maternally concordant to the total
291 number of sites. We also examined mitonuclear hybrid lines for the presence of paternally
292 inherited mtDNA. This was accomplished by mapping trimmed and paired sequence reads to the
293 reference genome as well as all mtDNA haplotypes simultaneously. We measured depth of
294 coverage using samtools depth command to identify any potential sources of contamination.

295

296

Results

DNA sequencing

Illumina HiSeq 4000 sequencing yielded an average of 34.7 million reads for mitonuclear hybrid line pools, and 76.1 million reads for inbred line pools. Following quality trimming and mapping of paired reads to the appropriate references, an average of 29 million reads mapped for cybrid pools, and 61 million reads mapped for maternal and paternal line pools. Average nuclear genome coverage across inbred lines was 91.88% at a mean depth of coverage of 26x. Across the mitochondrial genome, the mean depth of coverage was 2670X, and genome coverage was 100%. Nuclear divergence (F_{ST}) between paternal lines ranged from 0.049 to 0.369 in lines with BR nDNA, and from 0.102 to 0.378 in lines with SD nDNA (Figure 1C). Mitochondrial divergence (d_{XY}) between parental lines ranged from 0.7% to 21.1% in BR nDNA lines, and 9.6% to 20.6% in SD nDNA lines. The mitonuclear hybrid panel represented a wide range of mitochondrial variation, with as few as 13 amino acid substitutions between the BR and LJ mitotypes, 170 aa substitutions between the BR and SD nuclear line mitotypes, and 555 aa substitutions between SD and FHL haplotypes. The highly divergent FHL haplotype also differed from the BR & LJ haplotypes by 546 aa substitutions.

For each mitonuclear hybrid line, we measured allele frequencies at an average of 580k divergent nDNA SNPs between parental lines. We found that alleles were mostly concordant with paternal nDNA, with limited evidence of introgression from maternal nDNA, with paternal concordance rates ranging from 99.15% - 100% (Figure 1C). To test for potential mtDNA contamination via paternal leakage or experimental error, we compared depth of coverage across

318 all mtDNA haplotypes, since mtDNA positions and alleles are not comparable across haplotypes.
319 We found that the percent maternally matching depth ranged from 94.09% to 99.81%, while the
320 percent of paternally matching depth ranged from 0.02% to 0.28% providing limited evidence
321 for contaminating mtDNA (Figure 1C).
322
323 **Trait measurements and modeling**
324 Despite initially setting up four replicates for each mitonuclear hybrid line, low productivity led
325 to extinction of several replicates, forcing us to proceed with one replicate per line to keep our
326 experiment balanced. We measured the hatching number for 182 females coming from 41
327 families reared at 15ºC and 216 females from 40 families reared at 25ºC. Male remating success
328 was measured for 491 males, using a total of 2,458 wild-caught females. Since 378 females died
329 over the course of the experiment, we discarded 31 males that had fewer than four out of six
330 females remaining in order to reduce variation associated with differential access to females.
331 Therefore, our male remating experiment is based on 235 males from 68 families reared at 15ºC
332 and 225 males from 76 families reared at 25ºC. The average male successfully copulated with
333 2.45 females in the span of 14 days when reared at 15°C, declining to 2.04 females at 25°C
334 representing a 17% reduction. In the average female clutch, 30.05 eggs hatched at 15°C,
335 declining to 21.50 eggs hatching at 25°C representing a 28% reduction. Female hatching number
336 declined an average of 31.16% in mitonuclear hybrid lines when females were bred with siblings
337 as opposed to wild-caught males (Document S1, Figure S2. Lifespan, frailty, and rate of
338 senescence was measured for 3,072 individuals, with 1,531 individuals from 89 families reared
339 at 15ºC, and 1,541 individuals from 77 families reared at 25ºC.
340

341 Experiments on early developmental stages indicate that mortality rate occurring before sexual
342 maturity was very high, ranging from 14.6% to 90.6% mortality depending on cross and
343 temperature (Document S1, Figure S1. Naupliar stages had the highest mortality, ranging from
344 4.2% to 84.4%, while copepodid stages ranged from 1.5% to 27.9% mortality. Linear mixed-
345 effects modeling showed that measurements describing the development rate varied significantly
346 with mtDNA x nDNA interactions and rearing temperature, with rates increasing at higher
347 temperature.
348

349 **Sex-effect modeling**

350 Model contrasts revealed mostly male-biased values for longevity (longer lifespan), and mixed
351 bias for fertility with three out of five contrasts being female biased (higher relative fertility)
352 (Figure 2A). Model selection comparing the four sex-effects models (Table S1) revealed the
353 prevalence of mtDNA x nDNA interactions, as models including three-way sex x nDNA x
354 mtDNA interaction term fit the data best in all temperature and trait combinations except for
355 relative fertility at 15°C, which was better fit with sex x nDNA interactions (ΔAIC = 17.35).
356 None of the sex-effects models uncovered significant sex x mtDNA interactions (Table S2).
357 However, we do see that sex x nDNA and sex x mtDNA x nDNA interactions are a significant
358 influence on fertility variation (Figure 2B).
359

360 **Mitonuclear coevolutionary status modeling**

361 We found that neither fertility nor longevity were influenced by mitonuclear status (matched vs.
362 mismatched), as indicated from type III ANOVA on fitted parameters (Table S3). Family sex
363 ratio was significantly influenced by mitonuclear status (χ^2= 17.95, p = 2.3e-5), as indicated in

364 linear mixed-effects modeling (Document S1, Figure S3), as well as nDNA x mitonuclear status
365 interactions (χ^2= 26.29, p = 2.9e-7). Results using mortality-corrected family sex ratio data were
366 also consistent with uncorrected family sex ratio. (Table S5).
367
368 **Best-fit models**
369 Temperature significantly impacted all traits by reducing their average values (Table S4).
370 Notably, mean longevity was reduced by 102 days in 25ºC, an almost 10 day decrease per degree
371 reduction. Variation in mtDNA strongly impacted female hatching number (χ^2= 20.36, p =
372 1.43e-4), but not male remating success (χ^2= 0.29, p = 0.9621) or longevity (χ^2= 6.86, p
373 =0.0764). Variation in nDNA strongly impacted longevity (χ^2= 24.48, p = 1.98e-5) but neither
374 measure of fertility (female hatching number: χ^2= 1.37, p = 0.2416; male remating success: χ^2=
375 0.15, p = 0.6991). Mitochondrial effects impacted fertility more than longevity (Figure 2C, χ^2=
376 43.90, p = 3.6e-11), while nuclear effects impacted both traits equally (χ^2 = 2.28, p = 0.1308).
377 While temperature negatively impacted both fertility and longevity, its effects on longevity were
378 significantly larger than on fertility (χ^2 = 23.39, p = 1.32e-6). Linear mixed-effects modeling of
379 family sex ratio indicated significant influence of temperature (χ^2 = 10.02, p = 0.0015), mtDNA
380 haplotype (χ^2 = 28.35, p = 3.1e-6), as well as interactions between mtDNA and nDNA (χ^2 =
381 31.98, p =1.6e-8) and temperature and nDNA (χ^2 = 29.94, p = 1.4e-6; Document S1, Figure S3).
382
383 **Parametric survivorship modeling**
384 Survivorship curves indicate a drastic reduction in longevity shifting from 15°C to 25°C, with
385 SD nDNA individuals having higher survivorship than BR nDNA individuals at 25°C (Figure
386 3A). Additionally, we see that median longevity is sex-biased in SD nDNA individuals reared at

387 15°C, with higher male longevity (Figure 3A insert, Wilcoxon rank sum test, p = 0.004). Rearing
388 temperature affected both frailty (χ^2= 22.55, p = 2.05e-6) and rate of senescence (χ^2= 23.27, p =
389 1.41e-6) in a similar manner, with the higher temperature leading to increased frailty and
390 increased rate of senescence (Table S6). Mitochondrial haplotype showed no significant
391 contribution to Gompertz parameters when reared at either 15ºC or 25ºC (Table S6). We found
392 significant sexual dimorphism in frailty and senescence in individuals reared at 25ºC, but not
393 those reared at 15ºC (Figure 3B). When reared at 25ºC, females had lower frailty than males, but
394 a higher rate of senescence and while this pattern held in both nDNA backgrounds, it was
395 nonsignificant in BR nDNA lines (Table S6).
396
397 **Mitochondrial coefficient of variation**
398 Females had significantly higher CV_{mt} than males in six out of eight temperature/nDNA/trait
399 groupings (Figure 4A, Table S3). For fertility in SD nDNA individuals reared at 25ºC, male and
400 female CV_{mt} was statistically indistinguishable (median difference = 5.6e-3, CI = (-1.9e-3, 1.2e-
401 2), p = 0.1212), while fertility in BR nDNA individuals at 25ºC showed higher male CV_{mt} than
402 females (median difference = -9.7e-2, CI = (-0.11, -0.09), p = 3.28e-94).
403
404 **Genetic correlation among haplotypes**
405 Intersexual correlations for median longevity (r = 0.99; CI_{95} = 0.21, 1.99) and fertility (r = 0.85;
406 CI_{95} = 0.07, 1.69) were significantly positive for both traits in BR nDNA individuals reared at 25
407 ℃, while the correlation for fertility in BR nDNA individuals was significantly negative (r = -
408 0.96; CI_{95} = -2.00, -0.14) in individuals reared at 15℃ (Figure 4B). The remaining intersexual
409 correlations were also positive ($0.05 \leq r \leq 0.86$) although 95% confidence intervals extended

410 into negative values indicating the presence of negative correlations among bootstrapped
411 replicates. For BR nDNA individuals, we found that intrasexual correlations between fertility
412 and longevity were significantly positive in females (hatching number vs median longevity: r =
413 0.90; CI_{95} = 0.06, 1.90) and males (remating success vs median longevity: r = 0.99; CI_{95} = -0.20,
414 2.04) reared at 25℃. Remaining intrasexual correlations were either positive (n = 4, $0.08 \leq r \leq$
415 0.61) or negative (n = 3, $-0.40 \leq r \leq -0.21$), yet had confidence intervals spanning zero,
416 indicating the presence of both positive and negative correlations among bootstrapped replicates
417 (Figure 4B).
418

419 ## Discussion

420 Our study sought to explicitly test three predictions arising from the mother's curse
421 hypothesis: higher mitochondrial genetic variance in males for fitness traits, negative intersexual
422 correlation among mitochondrial haplotypes for fitness traits, and higher impact of experimental
423 disruption of putatively coevolved mitonuclear genotypes on males. Our results did not support
424 these predictions. Females had a higher level of mitochondrial genetic variance in six tests,
425 equivalent variance in one test, and lower variance in one test (fertility in individuals with BR
426 nDNA reared at 25ºC). We also found little evidence for sexual antagonism for fertility or
427 longevity, with a significant negative intersexual correlation found in only one of eight tests
428 (fertility in BR nDNA at 15°C). Lastly, we did not find the significant influence of
429 coevolutionary status on fertility or longevity traits required to test the third prediction.
430

431 Detecting sex-bias in mitochondrial coefficient of variation for fitness traits is arguably
432 the most direct test of the hypothesis since it emphasizes the differential accumulation of
433 mutational variation between the sexes[74]. According to the mother's curse hypothesis,
434 mitochondrial mutations causing male infertility that are neutral in females are more likely to
435 spread in a population through random drift since males are a dead-end for natural selection on
436 mtDNA. However, this argument is best applied to randomly mating populations with no
437 inbreeding. In populations with even modest levels of inbreeding, such as those with
438 geographical population structure, females will also suffer fitness insults from mother's curse
439 mutations to a certain degree since they are more likely to mate with sub-fertile siblings[27,28,75].
440 The degree to which male subfertility influences female fertility fitness can also influence these
441 dynamics. In monandrous species like *Tigriopus*, females mate only once[76,77], resulting in a
442 direct relationship between male fertility and female offspring production. In this study, we
443 showed that female hatching number dropped substantially when mated with siblings compared
444 to wild-caught males, indicating the influence of male subfertility on female fertility. However,
445 in mating systems where females mate with several males (e.g. *Drosophila*), females can be
446 safeguarded against male infertility or subfertility[78]. As a result, selection to purge male-harming
447 mtDNA mutations is expected to be strongest in species with monandry and weakest with
448 polyandry whenever inbreeding is present[75]. Studies show that *T. californicus* avoid close
449 inbreeding[79], but live in highly isolated, ephemeral populations making inbreeding all but
450 inevitable[80,81]. Additionally, while inbreeding can limit mother's curse by decreasing the
451 conditions under which male-harming alleles can spread, it can also result in the spread of
452 female-harming alleles that benefit males and lead to female-biased fitness variance [22,27]. The
453 widespread female-biased fitness variance observed in our fertility and longevity experiments

454 may therefore indicate the impact of historical inbreeding on the fixation of mitochondrial
455 divergence sampled in our study.
456
457 We predicted that sex differences due to mitochondrial haplotype effects are greater for
458 fertility than longevity, based on the expectation that fertility genes are more sex-specific than
459 viability genes[82,83]. We also predicted that the consequences of mitonuclear mismatch should
460 increase with metabolic rate associated with increased temperature. Efficient energy production
461 depends on mitochondrial function, including mitonuclear coordination. Mild mitonuclear
462 mismatches may be tolerated under low aerobic demand and yet become lethal when energetic
463 demand become higher [40,but see 82]. Increased temperature reduced measures of both fertility and
464 longevity but was more dramatic with the latter. We uncovered significant mitonuclear effects
465 impacting longevity at 25°C but not 15°C. Additionally, we found that mitonuclear x sex effects
466 were significant for fertility at 25°C, but not 15°C. In general, mitochondrial haplotype effects in
467 our experiment impacted fertility more than longevity, however experiments on the larval stages
468 indicate a substantial amount of mortality, influenced by temperature and mitonuclear
469 interactions, occurring before sexual maturity. Because *T. californicus* sperm are amotile,
470 declines in male fertility are not attributed to loss of sperm motility – a key marker of male
471 sterility in organisms with flagellated, motile sperm. Instead, declines in male fertility in our
472 study are likely due to the number of mature spermatids in a spermatophore, the ability of sperm
473 to maintain homeostasis while residing in the female reproductive tract, or behavior.
474 Survivorship analysis indicates that mtDNA variation had an inverse impact on frailty
475 and senescence between the sexes, similar to the 'Strehler-Mildvan (S-M) relationship[85]. When
476 reared at 25ºC, females had lower frailty than males while also having a higher rate of

477 senescence, despite having similar median longevity. One explanation for this relationship is that
478 the preferential survival of the most-frail female *T. californicus* may lead to an increase in the
479 rate of senescence for females, since frail individuals are more susceptible to aging. Male *T.*
480 *californicus* typically have lower tolerance than females to a variety of stressors, including
481 temperature, and a greater transcriptomic response to oxidative stress[49,50,52,86,87].
482
483 **Conclusion**
484 We found that the functional mtDNA effects were highly context-dependent, being
485 influenced by the nuclear-background in which they were expressed, the temperature in which
486 individuals developed, and/or the sex of the individual. We explicitly sought to test the main
487 predictions of the mother's curse hypothesis, finding patterns opposite to those predictions.
488 Support for the mother's curse hypothesis has been highly mixed to date, both theoretically and
489 empirically, with many studies rejecting these predictions. While most studies directly testing
490 predictions of the mother's curse hypothesis have used *Drosophila*, the predominance of
491 maternal inheritance of mitochondria in eukaryotes allows for a taxonomically diverse
492 investigation of the generality of mother's curse. Particularly, diversity in mating system should
493 be considered for future studies, as the fitness of females that mate with only one male will be
494 strongly determined by the fitness of her mate when there is inbreeding. Furthermore, sperm
495 diversity (motile/amotile, storage/remating) should be highlighted in order to address the
496 relevance of various mutational insults to male fitness potentially harbored by mitochondrial
497 DNA. In light of the evidence presented here and elsewhere, we suggest that accumulation of
498 male-harming mitochondrial mutations may not be a generalizable phenomenon.
499

Acknowledgments

We are thankful to MacKenzie Partridge, Manuel Morales and Mi Rae Park for their help during the experiments and population maintenance. We also thank Ning Li and Scott Applebaum for their constructive criticisms and suggestions, which greatly improved the quality of the manuscript. The experiments reported here were supported by a grant (#1656048) from the National Science Foundation, Division of Environmental Biology, awarded to SE.

Author contributions

Conceptualization, S.E.; Methodology, E.T.W, B.A.F. and S.E.; Investigation, E.T.W, B.A.F, J.A.P; Writing – Original Draft, E.T.W; Writing – Review & Editing, E.T.W and S.E.; Funding Acquisition, S.E. and E.T.W; Resources, J.A.P, and E.T.W; Supervision, S.E. and E.T.W

Declaration of interests

The authors declare no competing interests.

516 # References

517 1. Yang, D., Oyaizu, Y., Oyaizu, H., Olsen, G. J. & Woese, C. R. Mitochondrial origins. *PNAS*
518 **82**, 4443–4447 (1985).
519 2. Gray, M. W., Burger, G. & Lang, B. F. Mitochondrial Evolution. *Science* **283**, 1476–1481
520 (1999).
521 3. Hedges, S. B., Blair, J. E., Venturi, M. L. & Shoe, J. L. A molecular timescale of eukaryote
522 evolution and the rise of complex multicellular life. *BMC Evol Biol* **4**, 2 (2004).
523 4. McBride, H. M., Neuspiel, M. & Wasiak, S. Mitochondria: More Than Just a Powerhouse.
524 *Current Biology* **16**, R551–R560 (2006).
525 5. Pagliarini, D. J. & Rutter, J. Hallmarks of a new era in mitochondrial biochemistry. *Genes*
526 *Dev.* **27**, 2615–2627 (2013).
527 6. Chandel, N. S. Mitochondria as signaling organelles. *BMC biology* **12**, 1 (2014).
528 7. Birsoy, K. *et al.* An Essential Role of the Mitochondrial Electron Transport Chain in Cell
529 Proliferation Is to Enable Aspartate Synthesis. *Cell* **162**, 540–551 (2015).
530 8. Santos, J. H. Mitochondria signaling to the epigenome: A novel role for an old organelle. *Free*
531 *Radical Biology and Medicine* **170**, 59–69 (2021).
532 9. Bar-Yaacov, D., Blumberg, A. & Mishmar, D. Mitochondrial-nuclear co-evolution and its
533 effects on OXPHOS activity and regulation. *Biochimica et Biophysica Acta (BBA) - Gene*
534 *Regulatory Mechanisms* **1819**, 1107–1111 (2012).
535 10. Lotz, C. *et al.* Characterization, design, and function of the mitochondrial proteome: from
536 organs to organisms. *J. Proteome Res.* **13**, 433–446 (2014).
537 11. Brown, W. M., George, M. & Wilson, A. C. Rapid evolution of animal mitochondrial
538 DNA. *Proc. Natl. Acad. Sci. USA* 5 (1979).

539 12. Lynch, M. Rate, molecular spectrum, and consequences of human mutation. *Proceedings*
540 *of the National Academy of Sciences* **107**, 961–968 (2010).
541 13. Lynch, M. & Blanchard, J. L. Deleterious mutation accumulation in organelle genomes.
542 *Genetics* **102/103**, 29–39 (1998).
543 14. Schmidt, T. R., Wu, W., Goodman, M. & Grossman, L. I. Evolution of nuclear-and
544 mitochondrial-encoded subunit interaction in cytochrome c oxidase. *Molecular Biology and*
545 *Evolution* **18**, 563–569 (2001).
546 15. Willett, C. S. & Burton, R. S. Evolution of Interacting Proteins in the Mitochondrial
547 Electron Transport System in a Marine Copepod. *Mol Biol Evol* **21**, 443–453 (2004).
548 16. Bazin, E., Glémin, S. & Galtier, N. Population Size Does Not Influence Mitochondrial
549 Genetic Diversity in Animals. *Science* **312**, 570–572 (2006).
550 17. James, J. E., Piganeau, G. & Eyre-Walker, A. The rate of adaptive evolution in animal
551 mitochondria. *Molecular Ecology* **25**, 67–78 (2016).
552 18. Barreto, F. S. *et al.* Genomic signatures of mitonuclear coevolution across populations of
553 Tigriopus californicus. *Nature Ecology & Evolution* **2**, 1250–1257 (2018).
554 19. Hood, W. R. *et al.* The Mitochondrial Contribution to Animal Performance, Adaptation,
555 and Life-History Variation. *Integrative and Comparative Biology* **58**, 480–485 (2018).
556 20. Wolstenholme, D. R. Animal Mitochondrial DNA: Structure and Evolution. in
557 *International Review of Cytology* (eds. Wolstenholme, D. R. & Jeon, K. W.) vol. 141 173–216
558 (Academic Press, 1992).
559 21. Frank, S. A. & Hurst, L. D. Mitochondria and male disease. *Nature* **383**, 224–224 (1996).
560 22. Smith, S. R. T. & Connallon, T. The contribution of the mitochondrial genome to sex-
561 specific fitness variance. *Evolution* **71**, 1417–1424 (2017).

562 23. Gemmell, N. J., Metcalf, V. J. & Allendorf, F. W. Mother's curse: the effect of mtDNA
563 on individual fitness and population viability. *Trends in Ecology & Evolution* **19**, 238–244
564 (2004).
565 24. Cardullo, R. A. & Baltz, J. M. Metabolic regulation in mammalian sperm: Mitochondrial
566 volume determines sperm length and flagellar beat frequency. *Cell Motility* **19**, 180–188
567 (1991).
568 25. Holyoake, A. J. *et al.* High incidence of single nucleotide substitutions in the
569 mitochondrial genome is associated with poor semen parameters in men. *International*
570 *Journal of Andrology* **24**, 175–182 (2001).
571 26. M. Florencia Camus, David J. Clancy, & Damian K. Dowling. Mitochondria, Maternal
572 Inheritance, and Male Aging. *Current Biology* **22**, 1717–1721 (2012).
573 27. Wade, M. J. & Brandvain, Y. REVERSING MOTHER'S CURSE: SELECTION ON
574 MALE MITOCHONDRIAL FITNESS EFFECTS. *Evolution* **63**, 1084–1089 (2009).
575 28. Unckless, R. L. & Herren, J. K. Population genetics of sexually antagonistic
576 mitochondrial mutants under inbreeding. *Journal of Theoretical Biology* **260**, 132–136 (2009).
577 29. Hedrick, P. W. REVERSING MOTHER'S CURSE REVISITED. *Evolution* **66**, 612–616
578 (2012).
579 30. Innocenti, P., Morrow, E. H. & Dowling, D. K. Experimental Evidence Supports a Sex-
580 Specific Selective Sieve in Mitochondrial Genome Evolution. *Science* **332**, (2011).
581 31. Camus, M. F., Wolf, J. B. W., Morrow, E. H. & Dowling, D. K. Single Nucleotides in the
582 mtDNA Sequence Modify Mitochondrial Molecular Function and Are Associated with Sex-
583 Specific Effects on Fertility and Aging. *Curr Biol* **25**, 2717–2722 (2015).

584 32. Camus, M. F. & Dowling, D. K. Mitochondrial genetic effects on reproductive success:
585 signatures of positive intrasexual, but negative intersexual pleiotropy. 10.
586 33. Wolff, J. N. *et al.* Evolutionary implications of mitochondrial genetic variation:
587 mitochondrial genetic effects on OXPHOS respiration and mitochondrial quantity change with
588 age and sex in fruit flies. *Journal of Evolutionary Biology* **29**, 736–747 (2016).
589 34. Carnegie, L., Reuter, M., Fowler, K., Lane, N. & Camus, M. F. Mother's curse is
590 pervasive across a large mitonuclear Drosophila panel. *Evolution Letters* **5**, 230–239 (2021).
591 35. Mossman, J. A., Tross, J. G., Li, N., Wu, Z. & Rand, D. M. Mitochondrial-Nuclear
592 Interactions Mediate Sex-Specific Transcriptional Profiles in Drosophila. *Genetics* **204**, 613–
593 630 (2016).
594 36. Mossman, J. A., Biancani, L. M. & Rand, D. M. Mitonuclear Epistasis for Development
595 Time and its Modification by Diet in Drosophila. *Genetics* (2016)
596 doi:10.1534/genetics.116.187286.
597 37. Immonen, E., Collet, M., Goenaga, J. & Arnqvist, G. Direct and indirect genetic effects
598 of sex-specific mitonuclear epistasis on reproductive ageing. *Heredity* **116**, 338–339 (2016).
599 38. Đorđević, M. *et al.* Sex-specific mitonuclear epistasis and the evolution of mitochondrial
600 bioenergetics, ageing, and life history in seed beetles: SEX-SPECIFIC MITONUCLEAR
601 EPISTASIS. *Evolution* **71**, 274–288 (2017).
602 39. Ashburner, M., Golic, K. G., Hawley, R. S., & others. *Drosophila: a laboratory*
603 *handbook.* (Cold spring harbor laboratory press, 2004).
604 40. Lane, N. The Costs of Breathing. *Science* **334**, 184–185 (2011).

605 41. Burton, R. S., Feldman, M. W. & Curtsinger, J. W. Population genetics of Tigriopus
606 californicus (Copepoda: Harpacticoida): I. Population structure along the central California
607 coast. *Marine Ecology Progress Series* 29–39 (1979).
608 42. Burton, R. S. Intraspecific Phylogeography Across the Point Conception Biogeographic
609 Boundary. *Evolution* **52**, 734–745 (1998).
610 43. Edmands, S. Phylogeography of the intertidal copepod Tigriopus californicus reveals
611 substantially reduced population differentiation at northern latitudes. *Molecular Ecology* **10**,
612 1743–1750 (2001).
613 44. Edmands, S. Heterosis and Outbreeding Depression in Interpopulation Crosses Spanning
614 a Wide Range of Divergence. *Evolution* **53**, 1757–1768 (1999).
615 45. Pritchard, V. L. & Edmands, S. THE GENOMIC TRAJECTORY OF HYBRID
616 SWARMS: OUTCOMES OF REPEATED CROSSES BETWEEN POPULATIONS OF
617 *TIGRIOPUS CALIFORNICUS*: *TIGRIOPUS CALIFORNICUS* HYBRID SWARMS.
618 *Evolution* **67**, 774–791 (2013).
619 46. Voordouw, M. J. & Anholt, B. R. Heritability of sex tendency in a harpacticoid copepod,
620 Tigriopus californicus. *Evolution* **56**, 1754–1763 (2002).
621 47. Foley, B. R., Rose, C. G., Rundle, D. E., Leong, W. & Edmands, S. Postzygotic isolation
622 involves strong mitochondrial and sex-specific effects in Tigriopus californicus, a species
623 lacking heteromorphic sex chromosomes. *Heredity* **111**, 391–401 (2013).
624 48. Alexander, H. J., Richardson, J. M. L., Edmands, S. & Anholt, B. R. Sex without sex
625 chromosomes: genetic architecture of multiple loci independently segregating to determine
626 sex ratios in the copepod *Tigriopus californicus*. *Journal of Evolutionary Biology* **28**, 2196–
627 2207 (2015).

628 49. Willett, C. S. Potential Fitness Trade-Offs for Thermal Tolerance in the Intertidal
629 Copepod Tigriopus Californicus. *Evolution* **64**, 2521–2534 (2010).
630 50. Kelly, M. W., Sanford, E. & Grosberg, R. K. Limited potential for adaptation to climate
631 change in a broadly distributed marine crustacean. *Proc Biol Sci* **279**, 349–356 (2012).
632 51. Leong, W., Sun, P. Y. & Edmands, S. Latitudinal Clines in Temperature and Salinity
633 Tolerance in Tidepool Copepods. *Journal of Heredity* **109**, 71–77 (2018).
634 52. Foley, H. B. *et al.* Sex-specific stress tolerance, proteolysis, and lifespan in the
635 invertebrate Tigriopus californicus. *Experimental Gerontology* **119**, 146–156 (2019).
636 53. Bartoń, K. *MuMIn: Multi-Model Inference*. (2020).
637 54. Lenth, R. V. *emmeans: Estimated Marginal Means, aka Least-Squares Means*. (2020).
638 55. Bates, D., Mächler, M., Bolker, B. & Walker, S. Fitting Linear Mixed-Effects Models
639 Using lme4. *Journal of Statistical Software* **67**, 1–48 (2015).
640 56. Fox, J. & Weisberg, S. *An R Companion to Applied Regression*. (Sage, 2019).
641 57. Gompertz, B. On the Nature of the Function Expressive of the Law of Human Mortality,
642 and on a New Mode of Determining the Value of Life Contingencies. (1815)
643 doi:10.1098/rspl.1815.0271.
644 58. Jackson, C. flexsurv: A Platform for Parametric Survival Modeling in R. *Journal of*
645 *Statistical Software* **70**, 1–33 (2016).
646 59. R Core Team. *R: A Language and Environment for Statistical Computing*. (R Foundation
647 for Statistical Computing, 2020).
648 60. Canty, A. & Ripley, B. D. *boot: Bootstrap R (S-Plus) Functions*. (2020).
649 61. Davison, A. C. & Hinkley, D. V. *Bootstrap Methods and Their Applications*. (Cambridge
650 University Press, 1997).

651 62. Arnholt, A. T. & Evans, B. *BSDA: Basic Statistics and Data Analysis*. (2017).

652 63. Bolger, A. M., Lohse, M. & Usadel, B. Trimmomatic: a flexible trimmer for Illumina
653 sequence data. *Bioinformatics* **30**, 2114–2120 (2014).

654 64. Dierckxsens, N., Mardulyn, P. & Smits, G. NOVOPlasty: de novo assembly of organelle
655 genomes from whole genome data. *Nucleic Acids Research* **45**, e18 (2017).

656 65. Bernt, M. *et al.* MITOS: Improved de novo metazoan mitochondrial genome annotation.
657 *Molecular Phylogenetics and Evolution* **69**, 313–319 (2013).

658 66. Lunter, G. & Goodson, M. Stampy: A statistical algorithm for sensitive and fast mapping
659 of Illumina sequence reads. *Genome Res.* **21**, 936–939 (2011).

660 67. Picard Tools - By Broad Institute. https://broadinstitute.github.io/picard/.

661 68. Li, H. A statistical framework for SNP calling, mutation discovery, association mapping
662 and population genetical parameter estimation from sequencing data. *Bioinformatics* **27**,
663 2987–2993 (2011).

664 69. Darling, A. E., Mau, B. & Perna, N. T. progressiveMauve: Multiple Genome Alignment
665 with Gene Gain, Loss and Rearrangement. *PLoS ONE* **5**, e11147 (2010).

666 70. Ranwez, V., Douzery, E. J. P., Cambon, C., Chantret, N. & Delsuc, F. MACSE v2:
667 Toolkit for the Alignment of Coding Sequences Accounting for Frameshifts and Stop Codons.
668 *Mol Biol Evol* **35**, 2582–2584 (2018).

669 71. Larkin, M. A. *et al.* Clustal W and Clustal X version 2.0. *Bioinformatics* **23**, 2947–2948
670 (2007).

671 72. Yang, Z. PAML 4: Phylogenetic Analysis by Maximum Likelihood. *Mol Biol Evol* **24**,
672 1586–1591 (2007).

673 73. Kofler, R. *et al.* PoPoolation: A Toolbox for Population Genetic Analysis of Next
674 Generation Sequencing Data from Pooled Individuals. *PLoS ONE* **6**, (2011).
675 74. Dowling, D. K. & Adrian, R. E. Challenges and Prospects for Testing the Mother's Curse
676 Hypothesis. *Integrative and Comparative Biology* **59**, 875–889 (2019).
677 75. Zhang, H., Guillaume, F. & Engelstädter, J. THE DYNAMICS OF MITOCHONDRIAL
678 MUTATIONS CAUSING MALE INFERTILITY IN SPATIALLY STRUCTURED
679 POPULATIONS: MITOCHONDRIA, MALE INFERTILITY & SPATIAL
680 STRUCTURE. *Evolution* **66**, 3179–3188 (2012).
681 76. Vittor, B. A. Effects of the environment of fitness-related life history characters in
682 Tigriopus californicus. (University of Oregon, 1971).
683 77. Burton, R. S. Mating system of the intertidal copepod Tigriopus californicus. *Marine*
684 *Biology* **86**, 247–252 (1985).
685 78. Singh, S. R., Singh, B. N. & Hoenigsberg, H. F. Female remating, sperm competition and
686 sexual selection in Drosophila. *Genet Mol Res* **1**, 178–215 (2002).
687 79. Palmer, C. A. & Edmands, S. Mate choice in the face of both inbreeding and outbreeding
688 depression in the intertidal copepod Tigriopus californicus. *Marine Biology* **136**, 693–698
689 (2000).
690 80. Burton, R. S. Genetic Evidence for Long Term Persistence of Marine Invertebrate
691 Populations in an Ephemeral Environment. *Evolution* **51**, 993 (1997).
692 81. Dybdahl, M. F. Extinction, recolonization, and the genetic structure of tidepool copepod
693 populations. *Evol Ecol* **8**, 113–124 (1994).
694 82. Orr, H. A. Genetics of sterility in hybrids between two subspecies of Drosophila.
695 *Evolution* **43**, 180–189 (1989).

696 83. Turelli, M. & Orr, H. A. Dominance, Epistasis, and the Genetics of Postzygotic Isolation.
697 *Genetics* **154**, 1663–1679 (2000).
698 84. Pichaud, N., Ballard, J. W. O., Tanguay, R. M. & Blier, P. U. Mitochondrial haplotype
699 divergences affect specific temperature sensitivity of mitochondrial respiration. *J Bioenerg*
700 *Biomembr* **45**, 25–35 (2013).
701 85. Strehler, B. L. & Mildvan, A. S. General theory of mortality and aging. *Science* **132**, 14–
702 21 (1960).
703 86. Li, N., Arief, N. & Edmands, S. Effects of oxidative stress on sex-specific gene
704 expression in the copepod Tigriopus californicus revealed by single individual RNA-seq.
705 *Comparative Biochemistry and Physiology Part D: Genomics and Proteomics* **31**, 100608
706 (2019).
707 87. Li, N., Flanagan, B. A., Partridge, M., Huang, E. J. & Edmands, S. Sex differences in
708 early transcriptomic responses to oxidative stress in the copepod Tigriopus californicus. *BMC*
709 *Genomics* **21**, 759 (2020).
710

711 # SUPPLEMENTAL INFORMATION

712 Supplemental Information includes one document, three figures, and six tables and can be found
713 with this article online at xxx.
714

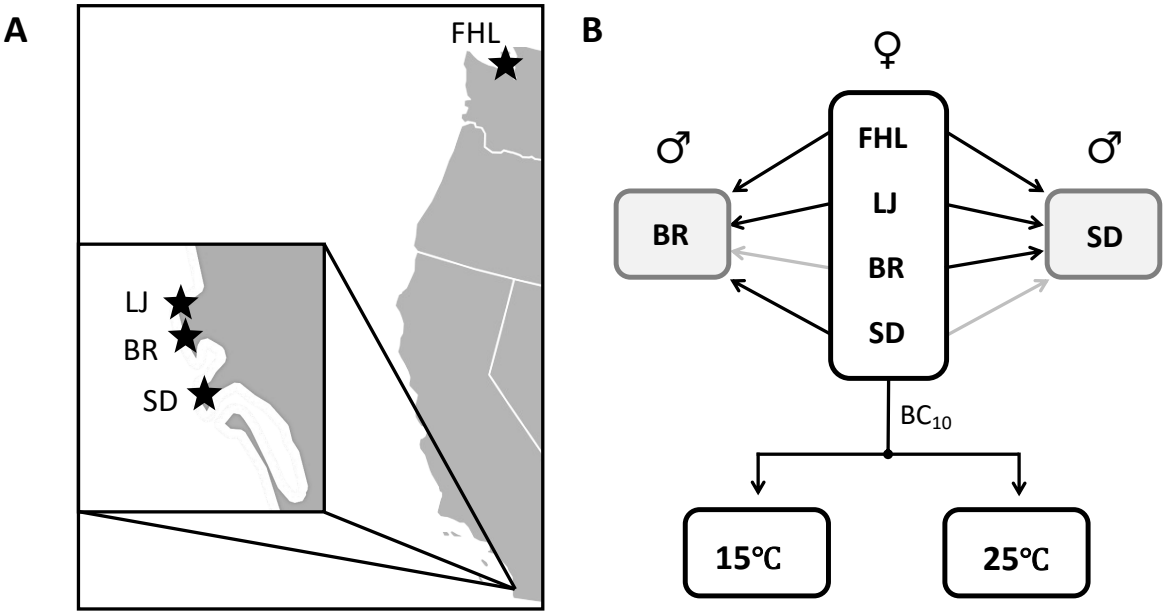

C

Backcross	Dam line	Sire line	Nuclear F_{ST}	mtDNA D_{XY}	mtDNA d_N	mtDNA d_S	% Paternal nDNA	% Maternal mtDNA	% Paternal mtDNA
SDxSD	SD	SD	0	0	0	0	100.00	94.09	94.09
BRxSD	BR	SD	0.102	0.096	0.023	0.532	99.90	97.22	0.28
LJxSD	LJ	SD	0.108	0.096	0.023	0.523	99.97	97.63	0.15
FHLxSD	FHL	SD	0.378	0.206	0.085	2.675	99.70	99.65	0.13
BRxBR	BR	BR	0	0	0	0	100.00	96.91	96.91
LJxBR	LJ	BR	0.049	0.007	0.002	0.046	99.93	95.96	0.08
SDxBR	SD	BR	0.102	0.096	0.023	0.532	99.72	95.32	0.02
FHLxBR	FHL	BR	0.369	0.211	0.085	4.347	99.15	99.81	0.02

Figure 1. Construction of mitonuclear hybrid panel

(A) Geographic location of populations used in this study – SD (San Diego, CA), BR (Bird Rock, CA), LJ (La Jolla, CA), FHL (Friday Harbor, WA). (B) Experimental design. Dams from the central panel were backcrossed to sires from BR and SD for 10 generations. Grey arrows indicate experimental control lines. Individuals from each line were reared at two contrasting temperatures, 15°C and 25°C. (C) DNA sequencing results from pool-seq. Measures of divergence (F_{ST}, D_{XY}, d_N, and d_S) were calculated between dam and sire line. Percent paternal nDNA and percent maternal/paternal mtDNA indicate minimal contaminating nDNA remaining in backcrossed individuals and the absence of paternal leakage of mtDNA.

715

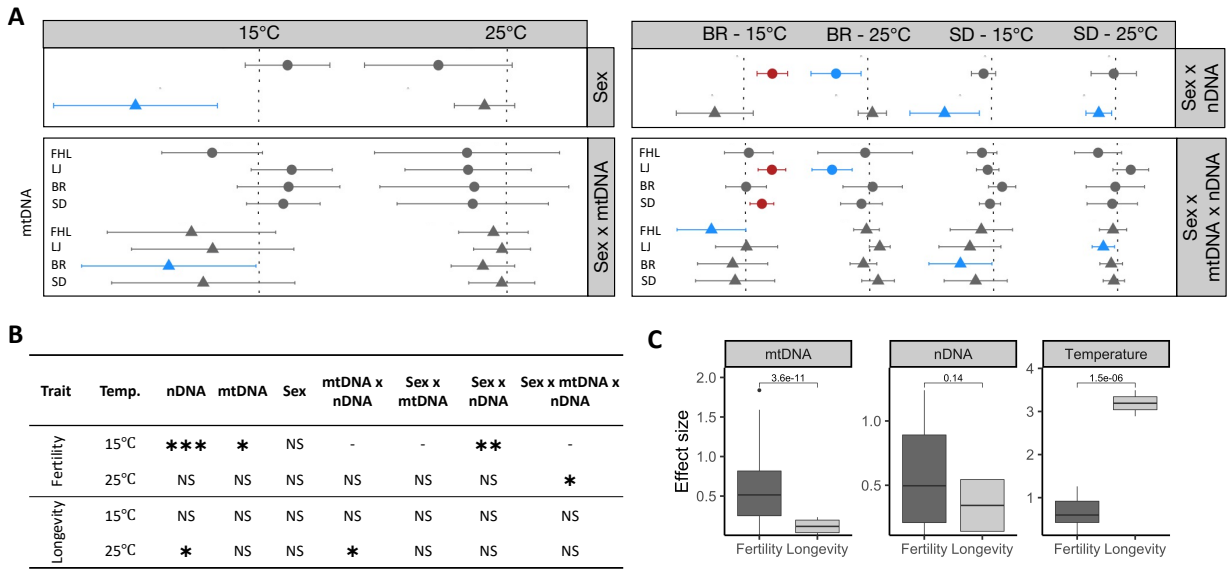

Trait	Temp.	nDNA	mtDNA	Sex	mtDNA x nDNA	Sex x mtDNA	Sex x nDNA	Sex x mtDNA x nDNA
Fertility	15°C	∗∗∗	∗	NS	-	-	∗∗	-
	25°C	NS	NS	NS	NS	NS	NS	∗
Longevity	15°C	NS	NS	NS	NS	NS	NS	NS
	25°C	∗	NS	NS	∗	NS	NS	NS

Figure 2. Trait modeling results.

(A) Model contrasts between the sexes were plotted for each sex-effect model (Sex, Sex x mtDNA, Sex x nDNA, and Sex x mtDNA x nDNA). Fertility contrasts are represented as circles and longevity contrasts as triangles. Points to the left of the dotted zero-line indicate a higher mean in males and those to the right of the line indicate higher mean in females. Significant contrasts were colored to indicate the sex with the higher mean - red (higher female) or blue (higher male).

(B) Sex-effect model type III ANOVA table. Each row represents a separate model, with columns representing modeled fixed effects. Cells are marked with a dash when a variable is not included in the model. Abbreviations: NS – non significant ($p < 0.05$), ∗ – $p \leq 0.05$, ∗∗ – $p \leq 0.01$, ∗∗∗– $p \leq 0.001$.

(C) Genetic and temperature effect size comparisons between fitness traits. We estimated Cohen's *d* for all pairwise contrasts among cross, temperature, and sex groupings. For fertility, we used our best-fit sex-specific fertility models (female hatching number and male remating

731 success). For longevity, we used our best-fit models. Significance was determined using two-
732 sample unpaired Wilcoxon rank sum tests with a two-sided alternate hypothesis and 95%
733 confidence intervals. Sample sizes for contrasts were mtDNA, n = 96; nDNA, n = 32; and
734 Temperature, n = 32.
735

736

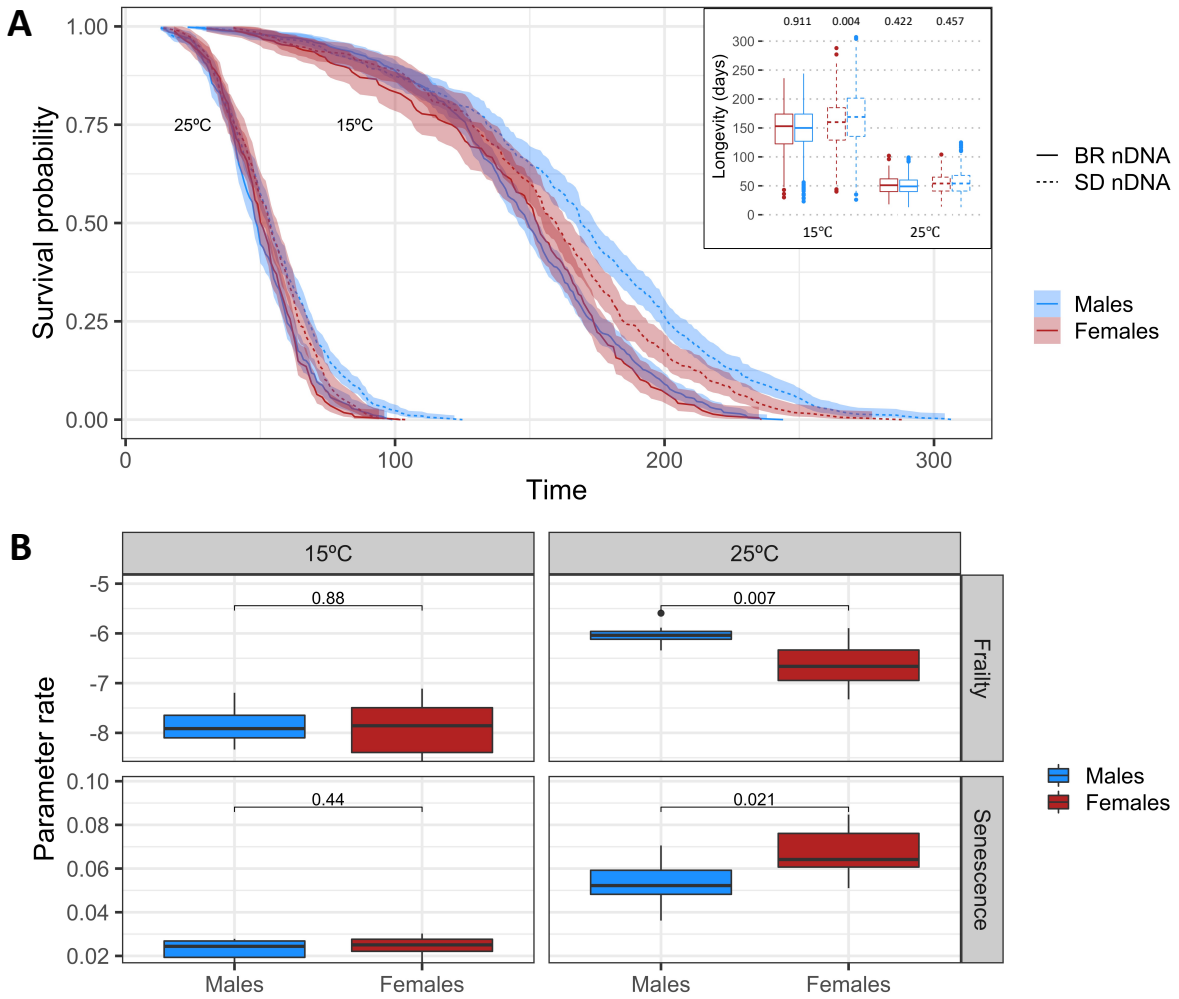

Figure 3. Males outlive females and have lower rates of senescence and higher frailty.

(A) Sex-specific survivorship curves based on nDNA and temperature groupings. Median longevity shown in insert with p-values indicating results of two-sample unpaired Wilcoxon rank sum tests with a two-sided alternate hypothesis and 95% confidence intervals.

(B) Sex contrasts for Gompertz parameters. We performed Wilcoxon tests as above to identify parametric differences in the rate of aging between the sexes.

737

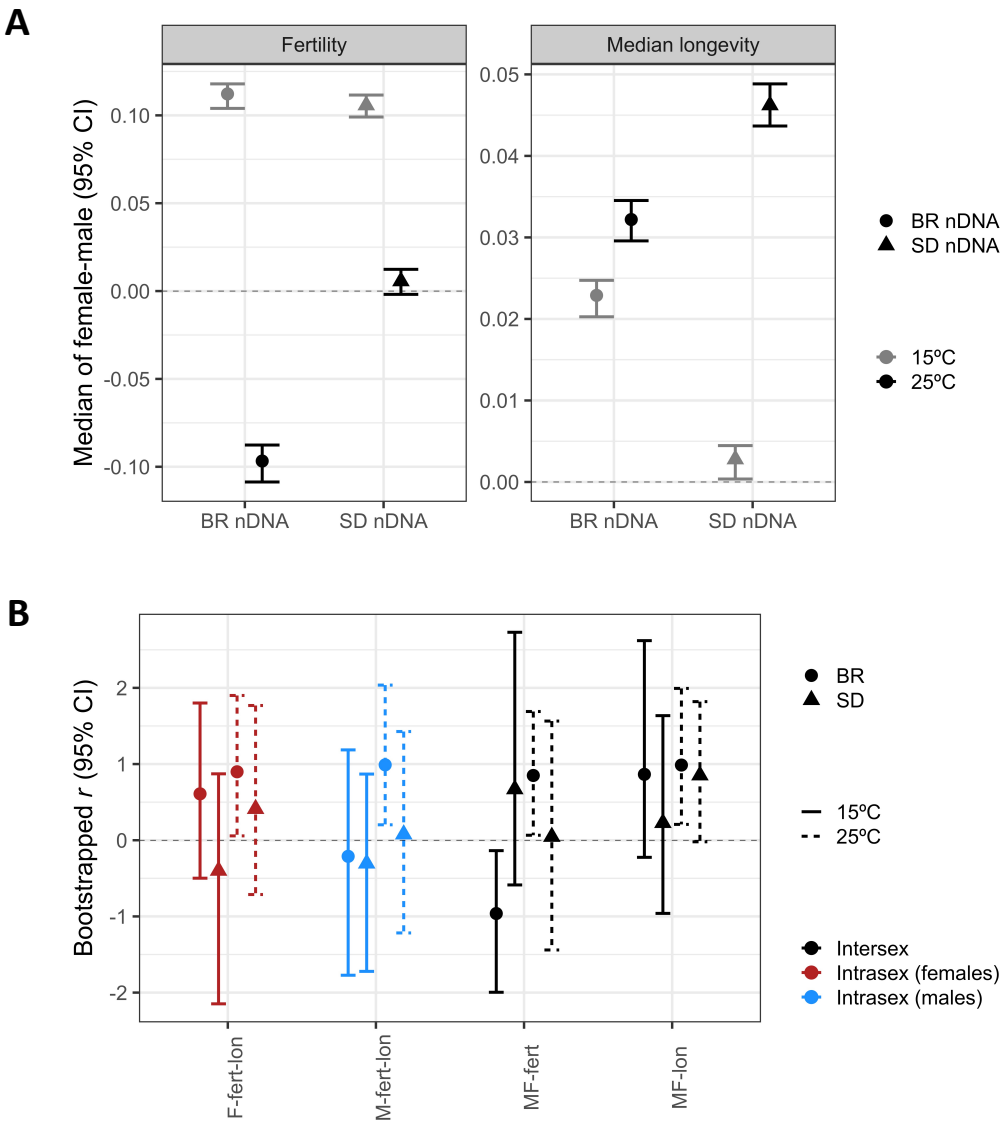

Figure 4. Testing the mother's curse hypothesis with mitonuclear hybrid *T. californicus.* (A) Sex differences in mitochondrial coefficient of variation (CV_{mt}) for fertility and longevity. We estimated CV_{mt} for both fertility and median longevity by temperature and nuclear line and performed a two-sided sign test on bootstrapped estimates (1000 samples). The sign test compares the difference between female and male median values with negative values indicating higher male CV_{mt}, while positive values indicate that females have higher $CV_{mt.}$. The majority

745 of groupings indicate higher mitochondrial genetic variation in females in contradiction to the
746 mother's curse hypothesis.
747 (B) Intra- and intersexual genetic correlation for female and male fertility and longevity across
748 mitochondrial haplotypes. Bootstrapped Pearson's correlation coefficients (95% confidence
749 intervals) were plotted for both rearing temperatures (15°C: solid lines, 25°C: dotted lines).
750 Abbreviations: F (females), M (males), fert (fertility: hatching number for females, remating
751 success for males), lon (mean longevity). The majority of intersexual correlations indicate
752 positive values, suggesting the absence of sexually antagonistic pleiotropy predicted by the
753 mother's curse hypothesis.
754